

# PROCEEDINGS OF SPIE

[SPIDigitalLibrary.org/conference-proceedings-of-spie](https://SPIDigitalLibrary.org/conference-proceedings-of-spie)

## Thermal behavior and management of membrane external-cavity surface-emitting lasers (MECSELs)








Hoy-My Phung, Philipp Tatar-Mathes, Aaron Rogers, Patrik Rajala, Sanna Ranta, et al.

Hoy-My Phung, Philipp Tatar-Mathes, Aaron Rogers, Patrik Rajala, Sanna Ranta, Hermann Kahle, Mircea Guina, "Thermal behavior and management of membrane external-cavity surface-emitting lasers (MECSELs)," Proc. SPIE 11984, Vertical External Cavity Surface Emitting Lasers (VECSELs) XI, 1198402 (4 March 2022); doi: 10.1117/12.2610644

**SPIE.**

Event: SPIE LASE, 2022, San Francisco, California, United States

# Thermal behavior and management of membrane external-cavity surface-emitting lasers (MECSELs)

Hoy-My Phung , Philipp Tatar-Mathes , Aaron Rogers , Patrik Rajala , Sanna Ranta , Hermann Kahle \*, and Mircea Guina 

Optoelectronics Research Centre (ORC), Physics Unit / Photonics, Faculty of Engineering and Natural Science, Tampere University, Korkeakoulunkatu 3, 33720 Tampere, Finland

## ABSTRACT

Thermal simulations based on the finite-element method provide an estimation of what the heat management in membrane external-cavity surface-emitting lasers (MECSELs) is capable of: When considering diamond and SiC heat spreaders, double-side cooling (DSC) leads to gain membrane temperatures that are about a factor two lower than with single-side cooling (SSC). For the thermally worse conductive sapphire, the temperature benefit from DSC can be up to four times lower than with SSC. Diamonds as heat spreaders are recommended over SiC if the power for pumping the gain membrane is three times larger, for instance at 30 W at a pump beam diameter of 180  $\mu\text{m}$ . Sapphire can be favored over SiC if the pump power is about five times lower, for instance at 2 W. Due to the limited lateral heat flow activity of sapphire, a smaller pump beam diameter of 90  $\mu\text{m}$  is suggested. A super-GAUSSIAN pump beam can be used instead of a GAUSSIAN pump beam to lower the gain membrane maximum temperature by a factor of three. Double-side pumping becomes significantly more important as soon as the gain membrane gets thicker than 1  $\mu\text{m}$ .

**Keywords:** MECSEL, semiconductor membrane lasers, thermal simulations, finite-element method, power scaling capability, diamond, SiC, sapphire, heat spreaders, double-side cooling, double-side pumping, pump beam geometry

## 1. INTRODUCTION

Membrane external-cavity surface-emitting lasers (MECSELs)<sup>1-4</sup> can be considered as a laser technology that offers a high-quality beam as like vertical-external-cavity surface-emitting lasers (VECSELs).<sup>4,5</sup> Wavelength versatility<sup>6-8</sup> is further advanced by the absence of a monolithically integrated distributed BRAGG reflector (DBR) in MECSELs. The central element is a gain membrane, which solely consists of a quantum well (QW) or quantum dot (QD) hetero structure. Placed within an open cavity, the gain membrane is optically pumped by an external pump source. As the energy conversion usually occurs from pump photons of higher energy into lower-energy MECSEL photons, a residual energy percentage is accumulated as heat in the gain membrane. For heat dissipation, the gain membrane is bonded between two transparent heat spreaders as shown in Fig. 1. With diamond as a heat spreader material, it has been shown that double-side cooling can be more effective than the single-side cooling approach.<sup>2</sup> The better thermal management allows the use of heat spreaders that have a lower thermal conductivity but are more cost-efficient, such as SiC<sup>9,10</sup> to scale up the output power into watt-level regions.<sup>11,12</sup> Furthermore, the possibility of double-side pumping<sup>13</sup> in MECSELs is a feature that can be used to pump thicker gain structures for longitudinal power scaling.

Thermal simulations about only a few specific issues with diamond as a heat spreader<sup>2,7</sup> have been performed to better understand the heat management and the power scaling potential. In this work, the thermal behavior with SiC, diamond, and sapphire is analyzed via the finite element method (FEM). The temperature behavior is compared among different heat spreader thicknesses, pump powers, and pump beam geometries. Also, the simulations reveal the relevance of double-side cooling as well as double-side pumping for gain membrane thicknesses from 500 nm to 2  $\mu\text{m}$ .

---

\*Further author information: Send correspondence to Hermann Kahle, E-mail: [hermann.kahle@tuni.fi](mailto:hermann.kahle@tuni.fi),

## 2. THERMAL MODEL FOR THE FINITE-ELEMENT METHOD

To simulate the temperature distribution over the gain membrane and the heat spreaders, COMSOL Multiphysics<sup>®</sup>, which is based on the finite-element method (FEM), was used.<sup>14–16</sup> Therefore, the simulations were conducted by dividing the gain membrane and heat spreader regions into meshes. Rotational symmetry in cylindrical coordinates allowed us to consider an excerpt along the radial  $r$  and axial  $z$  planes. The excerpt had a radius of 0.75 mm which corresponds to the heat sink aperture radius. As such, the heat sink mount itself was not part of the simulation. Thermal insulation was considered at the top and bottom heat spreader-air interfaces. Convection cooling effects were ignored. Instead, thermal insulation was considered. The temperature at the surfaces on the outer edge at  $r = 0.75$  mm of the cylindrical simulated volume were fixed at 20°.

In comparison with a 90  $\mu\text{m}$  large pump beam radius that was typically used in our experiments, the excerpt radius was large enough. To simplify the simulation, the individual layers of QWs and barriers/claddings and their spatial arrangement within the gain membrane were not separately considered. The gain membrane was simulated as a single barrier/cladding layer with a thickness of  $z_0$ . The temperature distribution was basically obtained from FOURIER heat equation in steady-state, as expressed as

$$-\left[\frac{\partial}{\partial r}\left(k_z\frac{\partial T}{\partial r}\right) + \frac{1}{r}k_r\frac{\partial T}{\partial r} + \frac{\partial}{\partial z}\left(k_z\frac{\partial T}{\partial z}\right)\right] = Q(r, z). \quad (1)$$

$k_r$  and  $k_z$  correspond to the thermal conductivities along the radial  $r$  and axial  $z$  coordinates, which might be different from each other due to the anisotropic heat flow. However, the anisotropy aspect was neglected since it affects the temperature rise by 2%, only.<sup>17</sup>  $T$  describes the temperature and  $Q(r, z)$  the generated heat distribution. The latter can be attributed to the quantum defect  $n_Q = 1 - \lambda_P/\lambda_{\text{MECSEL}}$  from optical pumping. Thus, for a GAUSSIAN pump beam geometry, the heat load can be described with

$$Q_{\text{GAUSS}}(r, z) = \frac{2 \cdot \eta_Q \cdot P_0}{\pi w^2} \cdot \alpha \cdot \exp\left(-\frac{2r^2}{w^2} - \alpha(z_0 - z)\right). \quad (2)$$

This quantity is the larger, the shorter the pump wavelength  $\lambda_P$  compared to the MECSEL lasing wavelength  $\lambda_{\text{MECSEL}}$  is. Furthermore, the pump power that arrives at the gain region is given by  $P_0$ , the  $1/e^2$  pump radius by  $w$ , and the pump absorption coefficient by  $\alpha$ . The gain membrane thickness  $z_0$  is implemented in Eq. 2, stating that the single-side pumping occurs from the  $z = z_0$  side.

## 3. GAIN MEMBRANE, COOLING AND PUMPING CONDITIONS

Figure 1 summarizes the parameter values used in the thermal simulations. The gain membrane was designed for an emission wavelength of  $\lambda_{\text{MECSEL}}$  and was  $\sim 550$  nm thick. It consisted of  $4 \times 3$  GaInAsP QWs, which were embedded in GaInP barrier/cladding layers. On both outer sides of the MECSEL structure, the window layers are made of AlGaInP. As 80% of the gain membrane consisted of GaInP, the single bulk layer approximation of GaInP was justified for the gain membrane. Thus, thermal conductivity corresponded to  $k_{\text{GaInP}} = 5.2$  W/m·K, calculated from VEGARD's law. A  $\lambda_P = 532$  nm GAUSSIAN pump laser was used in our experiments. The absorption coefficient at the pump wavelength was calculated from the pump power reflected and transmitted from the gain membrane. In both cases, sandwiched either between 4H-SiC or sapphire heat spreaders, the absorption coefficient was approximately  $\alpha = 5.7 \cdot 10^4$  cm<sup>-1</sup>. Although the pump light absorption from the heat spreaders was generally small, for SiC at 532 nm about 0.25 cm<sup>-1</sup>,<sup>9</sup> the absorption from the heat spreaders was included in  $\alpha$ . Furthermore, a bonding layer with a thickness of  $t_B = 100$  nm and a thermal conductivity of  $k_B = 0.4$  W/m·K was implemented between the gain membrane and the heat spreader on each side.

The thermal simulations were experimentally validated by the thermal resistance, obtained via spectral shift measurements in Fig. 2. At a pump beam diameter of  $d_P = 2 \cdot w = 180$   $\mu\text{m}$ , single-side pumped gain membrane, the emission wavelength shift rate with dissipated power was 0.85 nm/W, and with the heat sink temperature 0.20 nm/K. Correspondingly, the thermal resistance was about 4.25 K/W. Thus, the FEM model could be further applied to other heat spreader and pumping conditions.

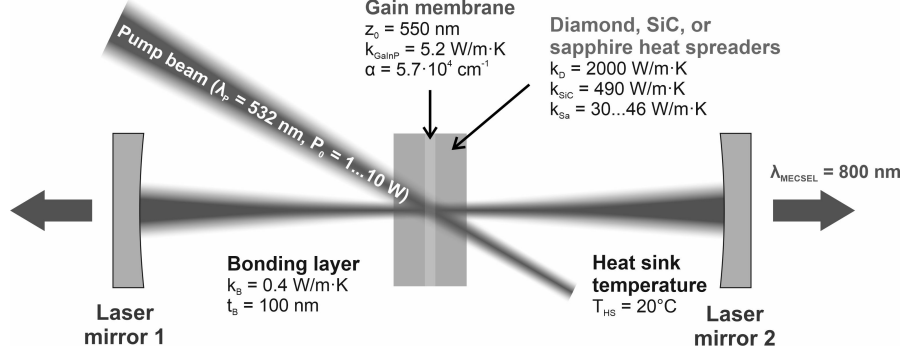


Figure 1. Schematic drawing of a MECSEL consisting of an open cavity and an optically pumped gain membrane, which is cooled by two intra cavity heat spreaders. Included are the parameter values used in the thermal simulations.

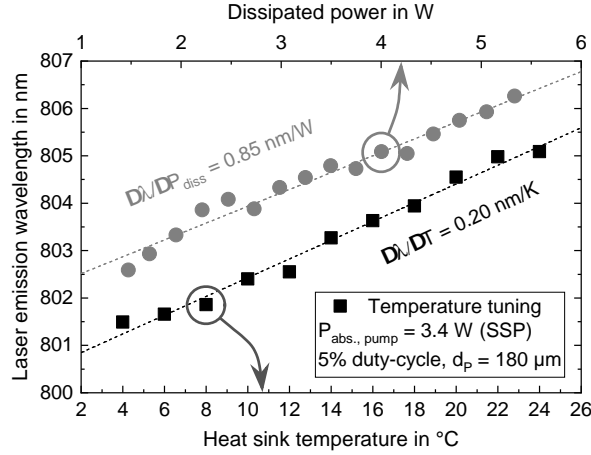


Figure 2. Central emission wavelength plotted against the dissipated power (grey dots) and heat sink temperature (black squares) for a SiC-cooled, single-side pumped 800 nm MECSEL to determine the thermal resistance.

#### 4. IMPACT OF DOUBLE-SIDE COOLING THE GAIN MEMBRANE

Dating back to 2015, the first lasing MECSELS<sup>2</sup> were demonstrated with a single-side cooled semiconductor membrane using diamond. At that time, the implementation of a second heat spreader was further motivated for a better heat extraction. Thermal simulations suggested that the maximum temperature with the double-side cooling (DSC) could be twice times lower than with single-side cooling (SSC). Then, an experimental comparison in output power was conducted with SiC heat spreaders. Most likely, the second heat spreader allows the increase of output power, which was 2.5 times higher than with SSC.<sup>9</sup>

The radial temperature distribution of the gain membrane at the pumped side  $z = z_0 = 550$  nm is plotted from the radial center  $r = 0$  in Fig. 3a for SSC and in Fig. 3b for DSC. As shown for various SiC heat spreader thicknesses from 100  $\mu$ m to 500  $\mu$ m, the temperature in this plane is the highest at  $r = 0$  owing to the power distribution of the GAUSSIAN beam. It is notably here that the highest temperature with DSC is about two times smaller than with SSC. For instance, the simulations suggest a highest temperature with DSC to be about 117°C and with SSC about 218°C in case of 300  $\mu$ m thick SiC heat spreaders. Thus, the thermal improvement shown in the simulations is in a good agreement with the experiments presented by YANG *et al.*<sup>9</sup>

Furthermore, Fig. 3c the axial temperature distribution across the gain membrane at  $r = 0$ . Worth noting here is that the gain membrane is optically pumped at  $P_0 = 10$  W and attached to a SiC heat spreader at  $z = 550$  nm, the gain membrane is 5°C and therefore not significantly cooler than the unpumped side.

According to the thermal simulations, the temperature benefit of DSC with diamond heat spreaders was similar

to SiC. With sapphire heat spreaders, the temperature was up to fourfold lower which was probably due to the worse thermal conductivity of sapphire (refer to the thermal conductivity values in Fig. 1).

For a gain membrane, double-side cooled with 300  $\mu\text{m}$  thick SiC heat spreaders, the temperature distribution is plotted in Fig. 3d for various pump powers  $P_0$  from 5 W to 25 W. As can be seen, the maximum temperature at  $r = 0$  raises by nearly equidistant steps of  $\sim 8.3^\circ\text{C}$  per watt.

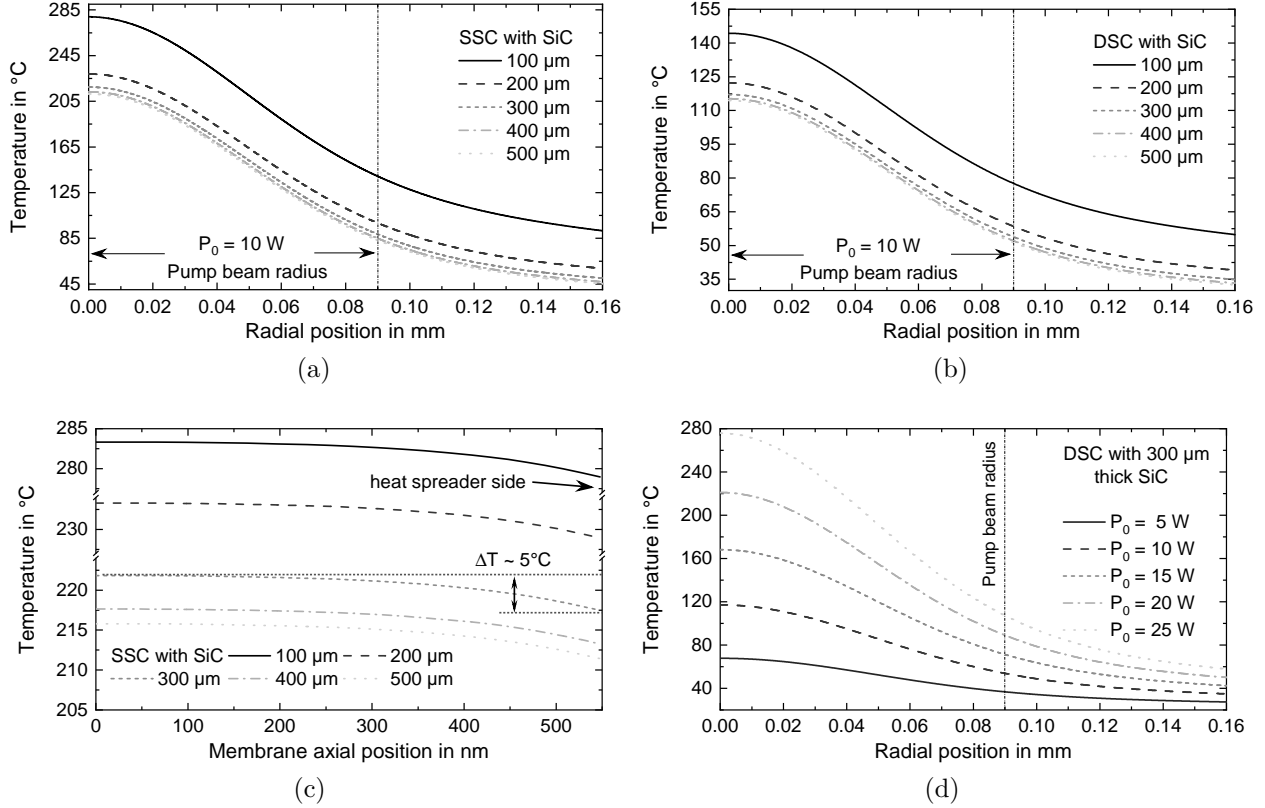


Figure 3. Temperature distribution on the pumped side of the gain membrane plotted from the radial center ( $r = 0, z = z_0 = 550 \text{ nm}$ ) with (a) SSC and (b) DSC. The gain membrane is single-side pumped with  $d_P = 180 \mu\text{m}$ . (c) Temperature distribution across  $z$  from the radial center of the SSC gain membrane at  $P_0 = 10 \text{ W}$ . (d) Radial temperature distribution for pump powers from 5 W to 25 W.

## 5. IMPACT OF HEAT SPREADER MATERIAL

With 300  $\mu\text{m}$  thick diamond heat spreaders, the radial temperature distribution of the gain membrane is plotted in Fig. 4a for a pump beam diameter of 180  $\mu\text{m}$ .

In comparison with Fig. 3b, the gain membrane heats up at  $r = 0$  to a maximum temperature of  $\sim 130^\circ\text{C}$  at three times higher pump power  $P_0 = 30 \text{ W}$ . Furthermore, the maximum temperature increases by  $\sim 28^\circ\text{C}$  for every 10 W step increase in pump power. In comparison with SiC, this is about three times smaller.

Compared with SiC<sup>18</sup> and diamond,<sup>19</sup> sapphire has a low thermal conductivity in the region between 30 W/m·K and 46 W/m·K.<sup>20</sup> Thus, the lateral heat flow ability is generally smaller to dissipate heat from the radial center of the pump beam to the outer side. A smaller pump beam diameter of 90  $\mu\text{m}$  and pump power regions up to 2 W have been considered in Fig. 4b. As can be seen, the simulation suggests that a maximum temperature of 130 W is achieved with a pump power of  $P_0 = 2 \text{ W}$ . The maximum temperature hereby increases by  $\sim 48^\circ\text{C}$  per watt.

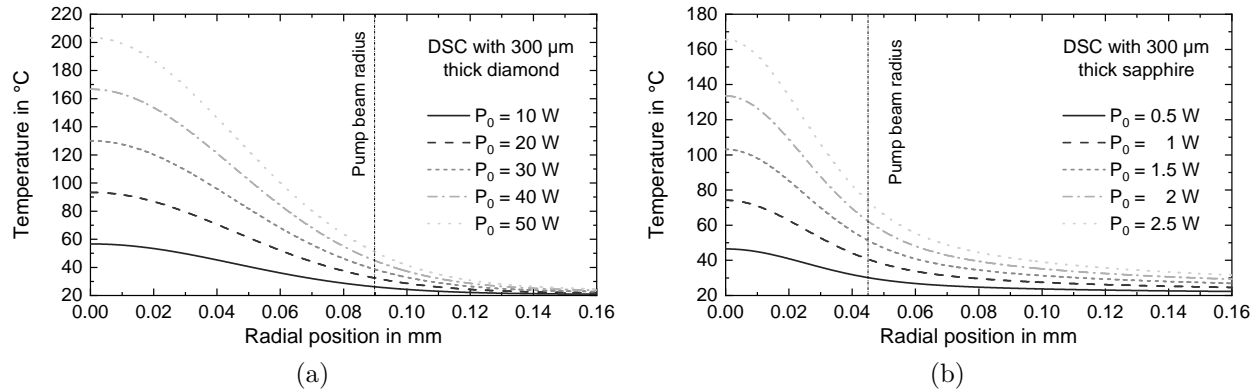


Figure 4. Temperature distribution on the single-side pumped side of the gain membrane plotted from the radial center ( $r = 0, z = z_0 = 550 \text{ nm}$ ). (a) With diamond heat spreaders for various  $P_0$  (b) With sapphire heat spreaders for various  $P_0$

## 6. IMPACT OF PUMP BEAM GEOMETRY

Alternatively, a super-GAUSSIAN profile can be considered for pumping the gain membrane. In comparison to a GAUSSIAN pump beam, its radial intensity distribution is more flat. Thus, the pump power is more equally distributed over the pump area, and the pump geometry is not only advantageous for the thermal management but also for single transversal mode operation<sup>21</sup> or thermal lensing. Such super-GAUSSIAN pump beam profiles are typically provided by fiber-coupled diode lasers. In the following thermal simulation a 10<sup>th</sup> order super-GAUSSIAN beam is considered with a heat load described as

$$Q_{\text{SG}, n=10}(r, z) \approx \frac{1.15 \cdot \eta_Q \cdot P_0}{\pi w^2} \cdot \alpha \cdot e\left(-2\left(\frac{r}{w}\right)^{10} - \alpha(z_0 - z)\right). \quad (3)$$

The outcome of the thermal simulation applying a super-GAUSSIAN pump beam with  $d_p = 180 \mu\text{m}$  is illustrated in Fig. 5.

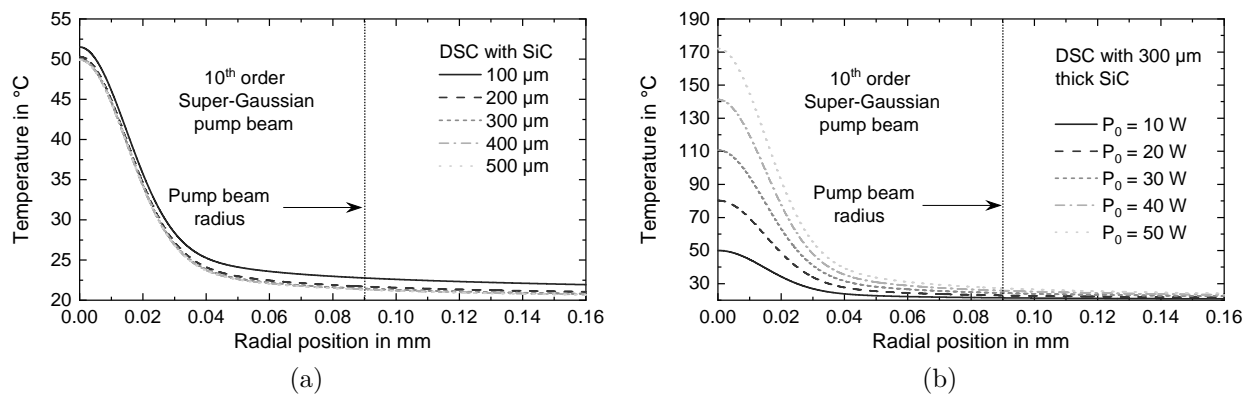


Figure 5. Temperature distribution on the single-side pumped side of the gain membrane plotted from the radial center ( $r = 0, z = z_0 = 550 \text{ nm}$ ) with a 10<sup>th</sup> order super-GAUSSIAN pump beam. (a) At  $P_0 = 10 \text{ W}$  for various SiC heat spreader thicknesses from  $100 \mu\text{m}$  to  $500 \mu\text{m}$ . (b) At a SiC heat spreader thickness of  $300 \mu\text{m}$  for various  $P_0$ .

At  $P_0 = 10 \text{ W}$ , the radial temperature distribution of the gain membrane at  $z_0 = 550 \text{ nm}$  is considered in Fig. 5a. For various SiC heat spreader thicknesses from  $100 \mu\text{m}$  to  $500 \mu\text{m}$  the maximum temperature is around  $51^\circ\text{C}$  at the radial center  $r = 0$ . Compared to the gain membrane pumped by a GAUSSIAN pump beam in Fig. 3b, the maximum temperature is at least two times lower. The overall better heat situation enables to pump the gain membrane at higher powers.

Figure 5b shows the radial temperature distribution of a gain membrane, double-side cooled by two 300  $\mu\text{m}$  thick SiC heat spreaders at pump powers from  $P_0 = 10\text{ W}$  to  $P_0 = 50\text{ W}$ . As can be seen, every 10 W step increase of pump power raises the maximum temperature by  $\sim 30^\circ\text{C}$ . Furthermore, the gain membrane can be pumped by a super-GAUSSIAN pump beam at  $P_0 = 30\text{ W}$  for a similar maximum temperature value of  $110^\circ\text{C}$  with a GAUSSIAN pump beam at  $P_0 = 10\text{ W}$ .

## 7. IMPACT OF DOUBLE-SIDE PUMPING THE GAIN MEMBRANE

So far, the thermal simulations have only considered single-side pumping (SSP) of the gain membrane. From Beer-Lambert law it follows that the intensity of any kind of irradiation penetrating through an absorbing matter drops exponentially over the distance, and so also the pump light absorbed within the gain membrane. Especially for thick gain membranes, the inhomogeneous pump intensity distribution matters since it is probable that the pump light does not arrive at the backside region of the membrane. This leads to unpumped regions that lower the operation efficiency.

A way to create a more homogeneous pumping would be double-side pumping (DSP) the gain membrane.<sup>13,22</sup> How DSP affects the temperature across gain membranes with thicknesses of 500 nm, 1  $\mu\text{m}$ , and 2  $\mu\text{m}$ , is illustrated in Fig. 6.

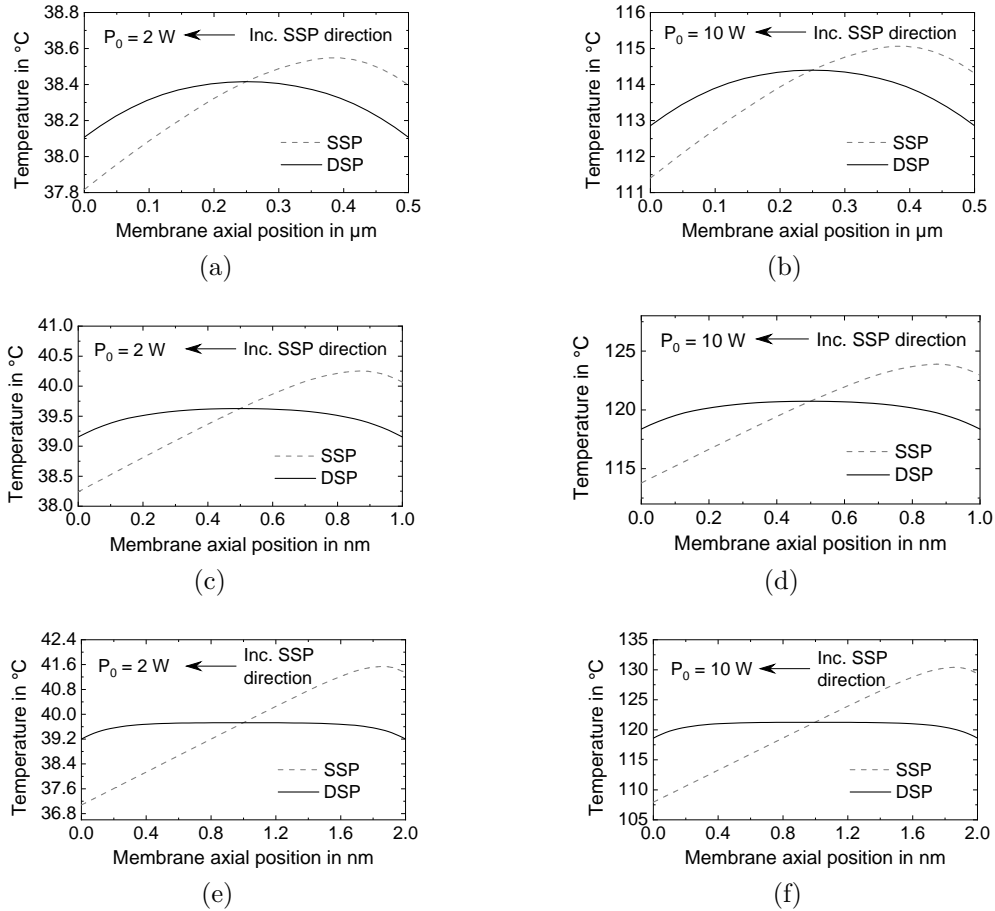


Figure 6. Membrane temperature distribution plotted across the axial direction at  $r = 0$  for SSP and DSP, various membrane thicknesses and incident pump powers. The gain membrane is cooled between two 350  $\mu\text{m}$  thick SiC heatspreaders at  $d_P = 180\text{ }\mu\text{m}$ . For a 500 nm thick gain membrane at (a)  $P_0 = 2\text{ W}$  and (b)  $P_0 = 10\text{ W}$ , for a 1  $\mu\text{m}$  thick gain membrane at (c)  $P_0 = 2\text{ W}$  and (d)  $P_0 = 10\text{ W}$ , and for a 2  $\mu\text{m}$  thick gain membrane at (e)  $P_0 = 2\text{ W}$  and (f)  $P_0 = 10\text{ W}$ .

In all six scenarios in Fig. 6, the temperature distribution across the axial membrane position  $z$  is flatter with



DSP than with SSP. In case of SSP, the highest temperature is not at  $z = z_0$  direct next to the heat spreader, but at about 150 nm more in the inner side of the gain membrane. The difference of the lowest and highest temperature at a relatively low pump power of  $P_0 = 2$  W is between 1°C and 5°C with SSC. In contrast, the temperature difference is less than 1°C with DSC.

Figures 6b, 6d, and 6f show the temperature distribution at  $P_0 = 10$  W. For thicker, single-side pumped gain membranes, the temperature difference becomes larger with the membrane thickness: At  $z_0 = 500$  nm, the difference is about 4°C, at  $z_0 = 1$  μm about 10°C, and  $z_0 = 2$  μm about 23°C, respectively. Thus, DSP can be relevant for gain structures thicker than  $\sim 1$  μm. On the other hand, the temperature of a double-side pumped gain membrane is generally lower and has a smaller difference of less than 3°C.

## 8. SUMMARY

The thermal behavior of MECSELS has been simulated via FEM and investigated under different kind of aspects that could be relevant for further power scaling this semiconductor laser technology in the future.

1. Double-side cooling of the gain membrane using SiC or diamond leads to lower temperatures than with single-side cooling. It has been found that the benefit is about a factor two.
2. For a 550 nm thick gain membrane, pumped by a GAUSSIAN-shaped pump beam with an  $1/e^2$  diameter of 180 μm, the maximum temperature increases with  $\sim 8.3^\circ\text{C}$  per watt with SiC and  $\sim 2.8^\circ\text{C}$  per watt with diamond. With sapphire heat spreaders, a worse lateral heat flow ability has been considered. Consequently, a smaller pump beam diameter of 90 μm and a lower pump power region up to 2.5 W have been taken into account. The maximum temperature hereby raises by 48°C per watt.
3. Furthermore, pumping the gain membrane with a 10<sup>th</sup> order super-GAUSSIAN pump beam has been considered. Since its pump beam shape is flatter than of a GAUSSIAN pump beam, the gain membrane temperature increases at a lower rate. If a SiC-cooled gain membrane is pumped by a GAUSSIAN beam at 10 W for instance, the maximum temperature is about 110°C. For the same temperature, the gain membrane can be pumped at 30 W with a super-GAUSSIAN beam.
4. Double-side pumping (DSP) has been compared with single-side pumping (SSP) for 0.5 μm, 1 μm, and 2 μm thick gain membranes at  $P_0 = 2$  W and  $P_0 = 10$  W. It has been found that DSP contributes to a more equally distributed temperature distribution across the gain membrane than with SSP. This is especially beneficial for gain membranes thicker than 1 μm pumped at higher pump powers over 10 W to maintain a symmetric cooling.

## ACKNOWLEDGMENTS

The authors would like to thank the Academy of Finland (No. 326455), PREIN Flagship Programme (No. 320165), Horizon 2020 Marie Skłodowska-Curie Actions - NetLaS (No. 860807), the Magnus Ehrnrooth Foundation, and the Finnish Foundation for Technology Promotion for the financial support.

## REFERENCES

- [1] Iakovlev, V., Walczak, J., Gębski, M., Sokoł, A. K., Wasiak, M., Gallo, P., Sirbu, A., Sarzała, R. P., Dems, M., Czyszanowski, T., and Kapon, E., “[Double-diamond high-contrast-gratings vertical external cavity surface emitting laser](#),” *J. Phys. D: Appl. Phys.* **47**(6), 065104 (2014).
- [2] Yang, Z., Albrecht, A. R., Cederberg, J. G., and Sheik-Bahae, M., “[Optically pumped DBR-free semiconductor disk lasers](#),” *Opt. Express* **23**(26), 33164–33169 (2015).
- [3] Kahle, H., Mateo, C. M. N., Brauch, U., Tatar-Mathes, P., Bek, R., Jetter, M., Graf, T., and Michler, P., “[Semiconductor membrane external-cavity surface-emitting laser \(MECSEL\)](#),” *Optica* **3**(12), 1506–1512 (2016).
- [4] Jetter, M. and Michler, P., eds., [[Vertical External Cavity Surface Emitting Lasers: VECSEL Technology and Applications](#)], Wiley-VCH GmbH, 1<sup>st</sup> ed. (2021).



- [5] Guina, M., Rantamäki, A., and Härkönen, A., “[Optically pumped VECSELs: review of technology and progress](#),” *J. Phys. D: Appl. Phys.* **50**(38), 383001 (2017).
- [6] Jeżewski, B., Broda, A., Sankowska, I., Kuźmich, A., Golaszewska-Malec, K., Czuba, K., and Muszalski, J., “[Membrane external-cavity surface-emitting laser emitting at 1640 nm](#),” *Opt. Lett.* **45**(2), 539–542 (2020).
- [7] Broda, A., Jeżewski, B., Szymański, M., and Muszalski, J., “[High-Power 1770 nm Emission of a Membrane External-Cavity Surface-Emitting Laser](#),” *IEEE J. Quantum Electron.* **57**(1), 1–6 (2021).
- [8] Phung, H.-M., Tatar-Mathes, P., Paranthoën, C., Levallois, C., Chevalier, N., Perrin, M., Kerchaoui, A., Kahle, H., Alouini, M., and Guina, M., “[Quantum dot membrane external-cavity surface-emitting laser at 1.5  \$\mu\text{m}\$](#) ,” *Appl. Phys. Lett.* **118**(23), 231101 (2021).
- [9] Yang, Z., Follman, D., Albrecht, A. R., Heu, P., Giannini, N., Cole, G. D., and Sheik-Bahae, M., “[16 W DBR-free membrane semiconductor disk laser with dual-SiC heatspreader](#),” *Electron. Lett.* **54**(7), 430–432 (2018).
- [10] Mirkhanov, S., Quarterman, A. H., Kahle, H., Bek, R., Pecoroni, R., C. J. C. Smyth, Vollmer, S., Swift, S., Michler, P., Jetter, M., and K. G. Wilcox, “[DBR-free semiconductor disc laser on SiC heatspreader emitting 10.1 W at 1007 nm](#),” *Electron. Lett.* **53**(23), 1537–1539 (2017).
- [11] Phung, H.-M., Kahle, H., Penttinen, J.-P., Rajala, P., Ranta, S., and Guina, M., “[Power scaling and thermal lensing in 825 nm emitting membrane external-cavity surface-emitting lasers](#),” *Opt. Lett.* **45**(2), 547–550 (2020).
- [12] Priante, D., Zhang, M., Albrecht, A., Bek, R., Zimmer, M., Nguyen, C., Follman, D., Cole, G., and Sheik-Bahae, M., “[Demonstration of a 20-W membrane-external-cavity surface-emitting laser for sodium guide star applications](#),” *Electron. Lett.* **57**(8), 337–338 (2021).
- [13] Kahle, H., Penttinen, J.-P., Phung, H.-M., Rajala, P., Tukiainen, A., Ranta, S., and Guina, M., “[Comparison of single-side and double-side pumping of membrane external-cavity surface-emitting lasers](#),” *Opt. Lett.* **44**(5), 1146–1149 (2019).
- [14] Lindberg, H., Strassner, M., Gerster, E., Bengtsson, J., and Larsson, A., “[Thermal management of optically pumped long-wavelength InP-based semiconductor disk lasers](#),” *IEEE Journal of Selected Topics in Quantum Electronics* **11**(5), 1126–1134 (2005).
- [15] Kemp, A. J., Maclean, A. J., Hastie, J. E., Smith, S. A., Hopkins, J.-M., Calvez, S., Valentine, G. J., Dawson, M. D., and Burns, D., “[Thermal lensing, thermal management and transverse mode control in microchip VECSELs](#),” *Appl. Phys. B* **83**(2), 189–194 (2006).
- [16] Mateo, C. M. N., Brauch, U., Schwarzbäck, T., Kahle, H., Jetter, M., Abdou Ahmed, M., Michler, P., and Graf, T., “[Enhanced efficiency of AlGaInP disk laser by in-well pumping](#),” *Opt. Express* **23**(3), 2472–2486 (2015).
- [17] Kemp, A. J., Valentine, G. J., Hopkins, J.-M., Hastie, J. E., Smith, S. A., Calvez, S., Dawson, M. D., and Burns, D., “[Thermal management in vertical-external-cavity surface-emitting lasers: finite-element analysis of a heatspreader approach](#),” *IEEE J. Quantum Electron.* **41**(2), 148–155 (2005).
- [18] Qian, X., Jiang, P., and Yang, R., “[Anisotropic Thermal Conductivity of 4H and 6H Silicon Carbide Measured Using Time-Domain Thermoreflectance](#),” *Mater. Today Phys.* **3**, 70–75 (2017).
- [19] Hopkins, J.-M., Smith, S. A., Jeon, C. W., Sun, H. D., Burns, D., Calvez, S., Dawson, M. D., Jouhti, T., and Pessa, M., “[0.6 W CW GaInNAs vertical external-cavity surface emitting laser operating at 1.32  \$\mu\text{m}\$](#) ,” *Electron. Lett.* **40**(1), 30–31 (2004).
- [20] Dobrovinskaya, E. R., Lytvynov, L. A., and Pishchik, V., [*Sapphire: Material, Manufacturing, Applications - Properties of Sapphire*], 55–176, Springer US, Boston, MA (2009).
- [21] Laurain, A., Hader, J., and Moloney, J. V., “[Modeling and optimization of transverse modes in vertical-external-cavity surface-emitting lasers](#),” *J. Opt. Soc. Am. B* **36**(4), 847–854 (2019).
- [22] Tidwell, S. C., Seamans, J. F., Bowers, M. S., and Cousins, A. K., “[Scaling CW diode-end-pumped Nd:YAG lasers to high average powers](#),” *IEEE J. Quantum Electron.* **28**(4), 997–1009 (1992).